Dimensional Crossovers in A + B → 0 Reaction in Tubular Geometries

Ramon Reigada†

Department of Chemistry and Biochemistry 0340, University of California−San Diego, La Jolla, California 92093-0340

Katja Lindenberg*

Department of Chemistry and Biochemistry 0340 and Institute for Nonlinear Science, University of California−San Diego, La Jolla, California 92093-0340

Received: April 28, 1999; In Final Form: July 19, 1999

Diffusion-controlled A + B → 0 reactions in constrained geometries are well-known to obey nonconventional dimension-dependent kinetics. We investigate these kinetics in narrow *d*-dimensional tubes to study the crossovers from early time *d*-dimensional kinetics to eventual one-dimensional kinetics. We rely on a reaction−diffusion model that leads to analytically verifiable quantitative results. The crossover times are identified as those times at which the kinetic exponent exhibits maximum curvature and are shown to be universally given by $t_c = 0.034W^2/D$ where W is the width of the tube along a narrow direction and D is the diffusion coefficient of both species. Our procedure overcomes many of the statistical difficulties inherent in Monte Carlo simulations of this problem [Ahn, J.; Kopelman, R.; Argyrakis, P. *J. Chem. Phys*. **1999**, *110*, 2116].

1. Introduction

Diffusion-limited reactions in constrained geometries obey reaction kinetics that exhibit completely different exponents than do well-mixed systems. This behavior is well understood for a large variety of reactions, starting with the original system A + B → 0 first studied by Ovchinnikov and Zeldovich.[1,2] When there are initially equal densities of A and B present in a random distribution in an infinite system of dimension $d < 4$, the density $\rho(t)$ of either species decays asymptotically as $\rho(t) \sim t^{-d/4}$. The departure from the classical decay law $\rho(t) \sim t^{-1}$ is obviously dramatic in low dimensions and is due to the evolution of initial fluctuations in the local species densities into ever larger regions in which one or the other species is predominant. Only efficient mixing can overcome this evolution toward segregation, and diffusion is not sufficiently efficient in low dimensions.

Recent work[3−5] deals with reaction kinetics of various types and associated random walks in tubular geometries in which the system is very long in one dimension but small in the other(s). In these geometries the reactants or walkers at first "don't know" that they are moving in a confined space until they "become aware" of the confining walls, at which point one or more dimensions are effectively lost. Thus, it is expected that the kinetic behavior at early times is two-dimensional or three-dimensional (depending on the dimensionality of the tube) but that asymptotically it becomes typical of that of a one-dimensional system. There are a number of interesting crossovers in the time dependences of the reactant densities in such tubular spaces as a function of various parameters such as the tube width and the initial densities. For the A + B reaction Ahn et al.[5] present a kinetic phase diagram showing a schematic of the different regimes of behavior that are possible as a function of the width W (short directions) of a finite tube. For example, for a two-dimensional tube with very small W they show that the density as a function of time behaves classically up to a crossover time t_c that scales as $W^{\alpha'}$ after which the behavior is one-dimensional. For wider tubes there are two crossovers, the first from classical to two-dimensional behavior at a W-independent crossover time, followed by a crossover from two-dimensional to one-dimensional behavior at a time that scales as $t_c \sim W^{\alpha}$. They discuss the exponents α' and α in detail. In particular, for Euclidean tubes the crossover times from behavior characteristic of a higher dimension to one of lower dimension scale as $t_c \sim W^2$ (i.e., $\alpha = 2$).

To support these and other results, Ahn et al. carry out extensive Monte Carlo simulations on discrete cubic lattices. The results are presented as graphs of the time-dependent exponent μ (which they call $-f$) in the relation $\rho \sim t^{\mu}$. The exponent μ crosses over from one plateau value to another and perhaps another; each plateau value is identified as the exponent characteristic of a particular regime (e.g., two-dimensional plateau followed by one-dimensional plateau) with crossover times whose W-dependence is difficult to ascertain from these simulations other than to support consistency with previous results.[3,4] The simulations are done on large systems (several thousand lattice sites along the long direction, between 1 and 20 in the short directions) with many particles that have to be individually tracked, and averaged over many thousands of runs. Nevertheless, even their most accurate (and very CPU-intensive) results are rather noisy and exhibit unexplained behavior that may or may not be artifactual (we believe it is, as will be noted below).

In this paper we revisit this problem, that is, we study the kinetics of the stoichiometric A + B → 0 reaction in tubular spaces, but using methods that permit more accurate determination of some exponents and crossovers. In particular, we study the change in kinetic behavior in tubular geometries due to the reduction of dimensionality. We determine not only scaling behaviors with great accuracy, but we also determine *coefficients* (which turn out to exhibit surprising universality).

† Permanent address: Departament de Química-Física, Universitat de Barcelona, Avda. Diagonal 647, 08028 Barcelona, Spain.

10.1021/jp9914018 CCC: $18.00
Published on Web 09/23/1999

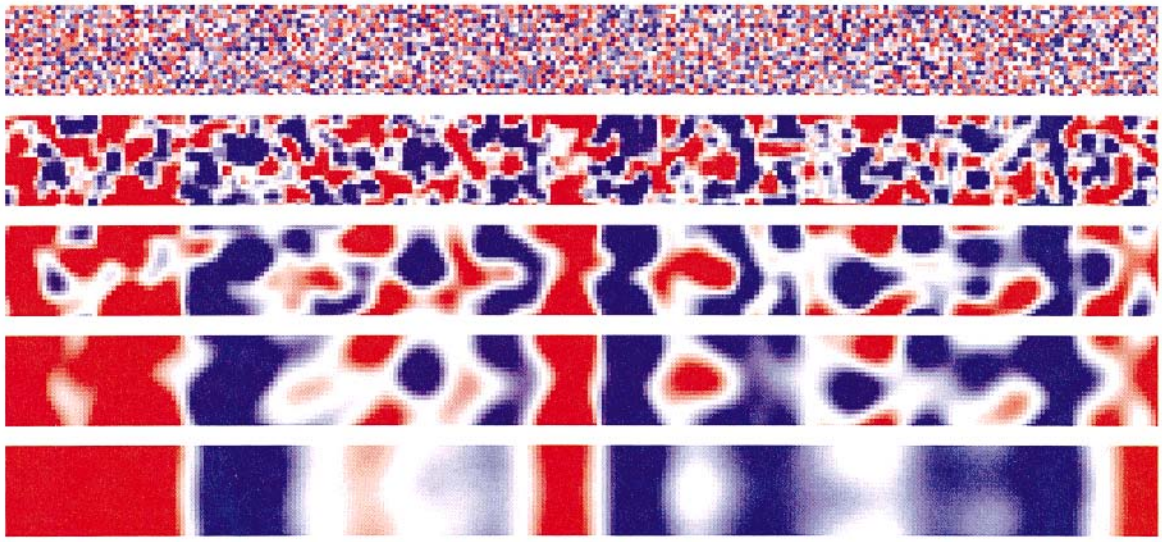

Figure 1. Time snapshots of the diffusion-limited reaction A + B → 0 in a narrow two-dimensional tube. The more abundant local density is shown in (A) red or (B) blue. At first the evolution follows two-dimensional OZ kinetics, but after some time (at around the time of the third or fourth snapshot) the evolution proceeds according to one-dimensional OZ kinetics.

In section 2 we present our model and discuss the particular quantities to be obtained from it. In section 3 we present our simulation results, which are further elucidated by a theoretical analysis in section 4. A short commentary on the overshoot artifacts of Ahn et al.[5] is also offered in section 3. We conclude with a summary in section 5.

2. The Model

The approach of Ahn et al. is microscopic. We rely on a more mesoscopic approach to the problem, namely the reaction−diffusion equations for the local densities $\rho_A(\mathbf{r},t)$ and $\rho_B(\mathbf{r},t)$:

$$\frac{\partial}{\partial t}\rho_A = D\nabla^2\rho_A - K\rho_A\rho_B$$

$$\frac{\partial}{\partial t}\rho_B = D\nabla^2\rho_B - K\rho_A\rho_B \qquad (1)$$

where D is the diffusion coefficient for both species and K is the local reaction rate constant. Although these continuum equations may fail on the very shortest time scales, shortest distances, and very low densities, they reproduce the kinetic features of the discrete microscopic system with remarkable accuracy on almost all scales[6] and are much easier and less costly to deal with numerically than the fully microscopic description.[7−9] A quantitative comparison of the results of integrating these coupled differential equations with those obtained from random walkers of types A and B on a discrete lattice that annihilate upon contact requires connection to be made between the lattice constant and time steps in the discrete problem and the parameters D and K in the continuum model.[6] As long as we are primarily interested in comparing scaling behavior, it is not necessary to dwell on this point other than to note that the discrete simulations correspond to the limit $K \rightarrow \infty$ for the reaction rate constant. In our simulations we take K to be very large, so large that its finite value is of little consequence for this discussion. Note that the global density $\rho(t)$ introduced earlier is just the integral of $\rho_A(\mathbf{r},t)$ or of $\rho_B(\mathbf{r},t)$ over the reaction volume.

A typical realization of the process obtained by numerical integration of the reaction−diffusion equations for a two-dimensional tubular space is shown in Figures 1 and 2. In Figure 1 reactant A is shown in red and reactant B in blue, and we see five consecutive time snapshots of the local densities. In each snapshot we show the color corresponding to the locally more abundant reactant. In order to observe the segregation process more explicitly, we show in Figure 2 the complementary map of reaction zones, namely, the product of the local concentrations, in levels of gray. The initial segregation pattern evolves well before the segregated clusters reach the boundaries: this is evident in the second snapshot. This initial segregation occurs according to two-dimensional Ovchinnikov−Zeldovich (OZ) kinetics characterized by the decay $\rho(t) \sim t^{-1/2}$. After some time, the clusters of A and B become comparable in size to the width of the tube. Beyond this time the further evolution of the system proceeds according to one-dimensional OZ kinetics $\rho(t) \sim t^{-1/4}$. The transition between these two regimes occurs at the so-called crossover time whose scaling behavior has motivated a considerable share of the previous work on the subject.

In this report we focus on the transitions between one OZ regime and another, namely, on transitions from OZ-2d to OZ-1d, from OZ-3d to OZ-1d, and from OZ-3d to OZ-2d. We do not analyze the situation (found for very narrow systems) where the transition occurs directly from the classical regime to the OZ regime of lowest dimensionality. In particular, we concentrate on the crossover times $t_{d_1 \rightarrow d_2}$ from OZ behavior associated with dimension d_1 to that associated with lower dimension d_2. These crossover times are obtained from density decay curves. We wish to establish the dependence of these crossover times on the width of the system and on the other parameters of the model, specifically the diffusion coefficient.

It is in fact straightforward (and correct) to argue that the crossover times should scale as

$$t_{d_1 \rightarrow d_2} \sim \frac{W^2}{D} \qquad (2)$$

This is a direct consequence of the fact that with free diffusion (which describes the local density difference between the two species[6]) the segregated zones grow in any direction as $\sqrt{Dt}$ and that the boundaries of the system will be perceived when this length is of the order of the tube width, $W \sim \sqrt{Dt}$. Although eq 2 is correct, it has been difficult to corroborate it

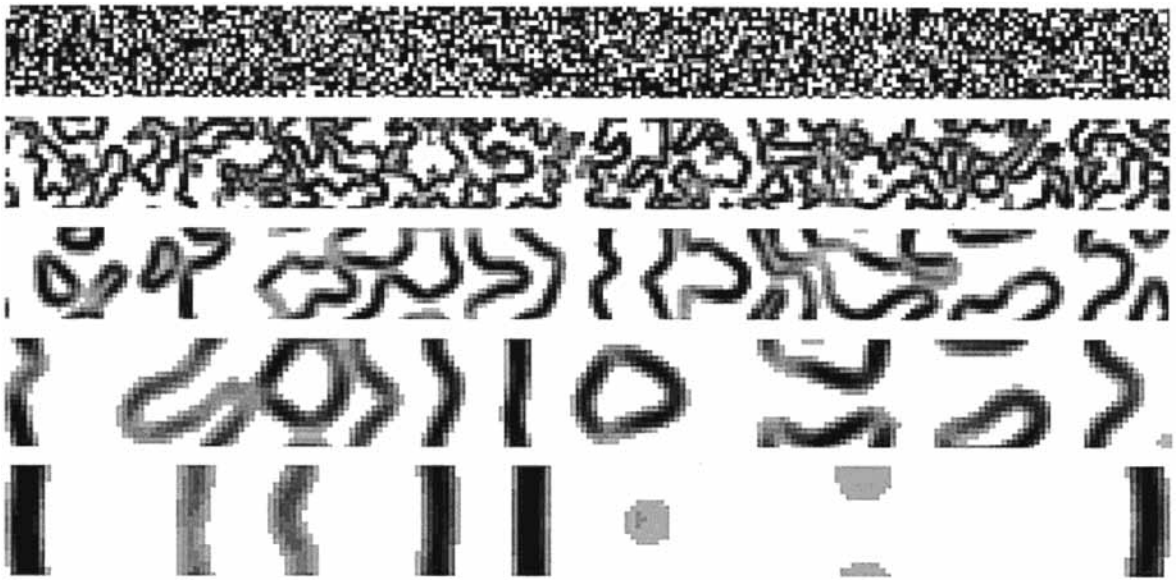

Figure 2. Reaction zones (product of local densities) in different levels of gray for the same system and the same snapshots as shown in Figure 1. Darker areas represent regions where the product is larger.

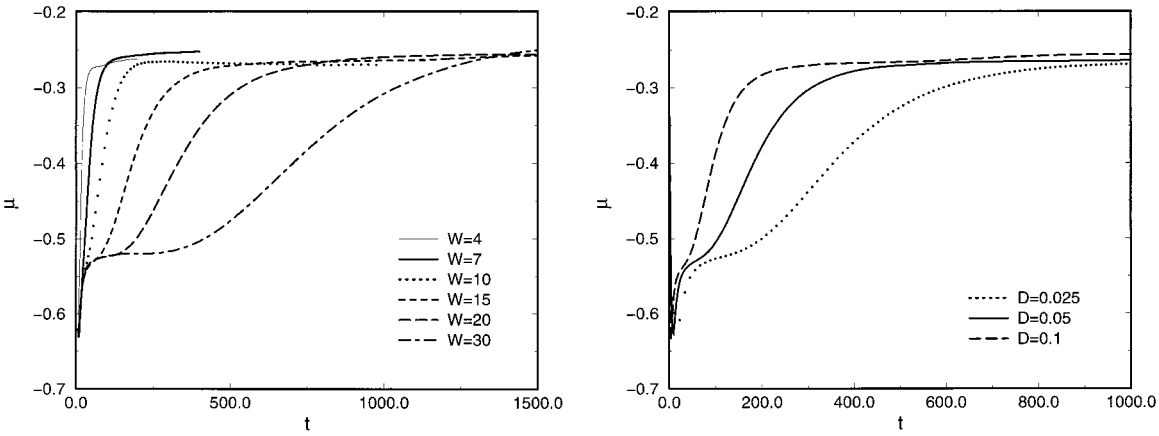

Figure 3. Exponent $\mu(t)$ as a function of time for narrow two-dimensional systems of length $L = 5000$ and width W. In the left part $D = 0.05$ is fixed and W is varied. In the right part $W = 15$ and D is varied. Each curve is an average over 10 realizations.

firmly from numerical simulations.[5] Furthermore, the coefficient in the relation has not been calculated or determined numerically. We shall do both using the reaction−diffusion model.

Our numerical solution of the reaction−diffusion model (eq 1) relies on a standard discrete scheme with a centered form for the Laplacian operator, a forward difference in time, and periodic boundary conditions. We take d-dimensional lattices and stoichiometric and randomly (absolutely uncorrelated) initial distributions for the reactants. In all the simulations shown in this work we take $K = 10$ and $\rho(0) = 1$. The discretization parameters are $\Delta t = 0.01$ and $\Delta x = 1$ and are small enough to ensure numerical convergence.

Lin and Kopelman[3] and also Ahn et al.[5] use reflecting rather than periodic boundary conditions along the shorter dimensionalities of the tubes. We have carefully ascertained within our model (and Li does as well within his random walk approach[4]) that this does not lead to any significant differences in the results.

The output of our numerical integrations yields the full time history of the decay of concentrations. We are specifically interested in the kinetic exponent μ. By following the temporal evolution of this exponent we can easily observe and identify how the kinetic behavior changes from one regime to another. We numerically compute μ in the following way:

$$\mu(t) = \frac{\mathrm{d}\log\rho(t)}{\mathrm{d}\log t} \Rightarrow \mu(t_i) \approx \frac{\log\rho(t_i) - \log\rho(t_{i-1})}{\log t_i - t_{i-1}} \quad (3)$$

3. Numerical Results

First we present our results for two-dimensional tubes and subsequently for three-dimensional ones.

We take our two-dimensional tubes to have a length $L = 5000$ and width W and carry out two series of calculations. In one we fix the diffusion coefficient $D = 0.05$ and vary W between 4 and 30. In the other we fix $W = 15$ and vary D from 0.025 to 0.1. The evolution of the resulting kinetic exponents $\mu(t)$ for both series is shown in Figure 3.

The following features are immediately apparent from these results: (i) The first plateau corresponds to the two-dimensional OZ regime. The kinetic exponent goes through a short "induction" period from the very early classical behavior ($\mu \sim -1$) in which the kinetics is dominated by the reaction of A and B densities initially in the same discretization cells toward this plateau. This induction period is D dependent but W independent. (ii) Two-dimensional OZ behavior ($\mu \approx -1/2$) persists for a longer time with increasing W. (iii) Increasing D leads to a shortening of the two-dimensional OZ interval (the process "arrives" at the boundaries more quickly). (iv) The transition

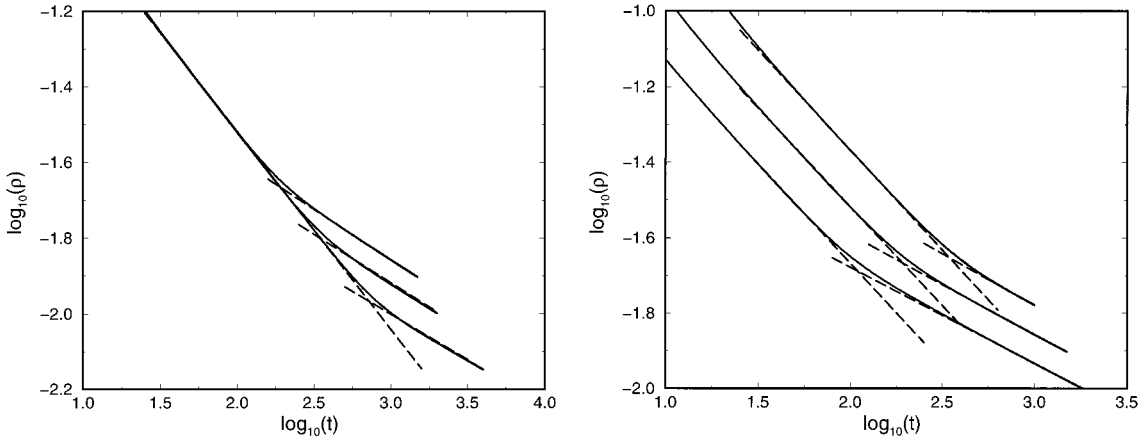

Figure 4. log−log plots of $\rho(t)$ vs time for the systems in Figure 3. The crossover times $t_{2\to1}$ from the two-dimensional OZ behavior (early times) to the one-dimensional OZ behavior (asymptotic times) are found from the intersection of the linear fits (dashed lines) in both regimes. Table 1 contains these results.

to the asymptotic one-dimensional OZ behavior ($\mu \approx -1/4$) is clear in all the simulations. (v) If W is too small there is a direct crossover from classical to one-dimensional OZ behavior with no passage through two-dimensional kinetics. This direct crossover is seen in our results for W below 10. Thus the critical width W_c to observe the transition between two OZ regimes is approximately 10 for our parameters. As noted earlier, we concentrate on the regime $W > W_c$ (W_c can be further decreased by choosing larger values for the reaction rate coefficient K and the initial density $\rho(0)$). (vi) The kinetic exponent in the two-dimensional OZ regime in our simulations is robust with respect to changes in W and D and is approximately equal to -0.52. The 4% deviation from the asymptotic OZ value $\mu = -1/2$ is due to the fact that K is finite in our model whereas the theoretical $-d/4$ exponent is obtained from an infinite local reaction rate (and, furthermore, it is an *asymptotic* exponent). We could diminish this difference by taking larger values for K. In any case, the deviation is very small in comparison with the noisy and nonrobust exponents obtained from the Monte Carlo simulations.[5]

Having established the clear presence of crossover behavior, we next wish to determine the crossover time $t_{2\to1}$ from two-dimensional to one-dimensional behavior. Lin and Kopelman[3] directly use concentration decay curves in their random walker analysis. They linearly fit the data of the temporal evolution of $\rho(t)^{-1} - \rho(0)^{-1}$ before and after the dimensional crossover and take the time at which the two linear fittings cross. This method leads to some "unexpected powers" when trying to scale $t_{2\to1}$ with W, and the authors recognize that this is probably not the optimal way to obtain the dimensional crossover times. To reconfirm the difficulties we apply the same procedure in Figure 4 to our two series of calculations. We collect the resulting intersections in Table 1 and observe that indeed this method is not suitable for our purposes: the variations in the scaled intersection are greater than 20% (and no other scaling does better).

A more robust measure of the dimensional crossover time is obtained as the time at which the exponent μ experiences its greatest change, i.e., the time at which the derivative $d\mu/dt$ has a maximum. Note that this measure is effective only with sufficiently noiseless and accurate data and would be impossible to implement using available Monte Carlo results. Figure 5 shows the derivative curves. The maxima of these curves can easily be determined with great accuracy and the results are also shown in Table 1. Clearly there is nearly perfect scaling: $t_{2\to1}D/W^2$ is essentially constant over all the runs.

TABLE 1: Crossover Times for Two-Dimensional Tubes Calculated from Linear Fit Intersections (Third Column) and for Two- and Three-Dimensional Tubes Calculated from the Maxima of the Derivatives of the Kinetic Exponents (Fourth, Fifth, and Sixth Columns)[a]

D	W	$(D/W^2)t_{2\to1}$, linear fits (Figure 4)	$(D/W^2)t_{2\to1}$, maximum derivative (Figure 5)	$(D/W^2)t_{3\to1}$, maximum derivative (Figure 8)	$(D/W_z^2)t_{3\to2}$, maximum derivative
0.050	30	0.040	0.036	0.035	
0.050	25				0.036
0.050	20	0.043	0.034	0.036	0.035
0.050	15	0.043	0.034	0.038	0.036
0.025	15	0.038	0.033	0.038	0.034
0.100	15	0.048	0.034	0.038	0.037

[a] In the sixth column W_z is the same as W in the second column, while $W_y = 40 =$ constant.

The most demanding test for the scaling properties of $t_{2\to1}$ is shown in Figure 6, where we redisplay all the results for $W > W_c$ shown in Figure 3 on a single graph of the exponent $\mu(t)$ as a function of the scaled variable tD/W^2. All the curves indeed collapse essentially onto a single curve that clearly displays the two-dimensional plateau at early times followed by a transition around the scaled time 0.034 toward the final one-dimensional plateau.

Next we consider three-dimensional tubular lattices of size $1000 \times W \times W$, that is, tubes of square cross section, and again carry out two series of calculations; in one we fix the diffusion coefficient and vary W, and in the other we fix W and vary D. The kinetic exponents for all cases exhibit a direct crossover from the three-dimensional plateau value of $-3/4$ to the one-dimensional exponent $-1/4$, and the scaling with D and W is again excellent. We show the scaled results for the exponents in Figure 7.

To determine the crossover times $t_{3\to1}$ from three-dimensional OZ behavior to one-dimensional OZ behavior, we again determine the maximum values of $d\mu/dt$. The derivative curves are shown in Figure 8, and their maxima are tabulated in Table 1. The scaled time is again nearly constant with a value of about 0.037 within a scatter of about $\pm 4\%$.

Finally, we consider three-dimensional tubular lattices but of rectangular cross section. The size of the lattice is $1000 \times W_y \times W_z$. By appropriate choices of W_y and W_z one can now observe two separate crossovers, one from OZ-3d to OZ-2d behavior and another subsequent one from OZ-2d to OZ-1d. We fix the value of $W_y = 40$ and carry out two series of

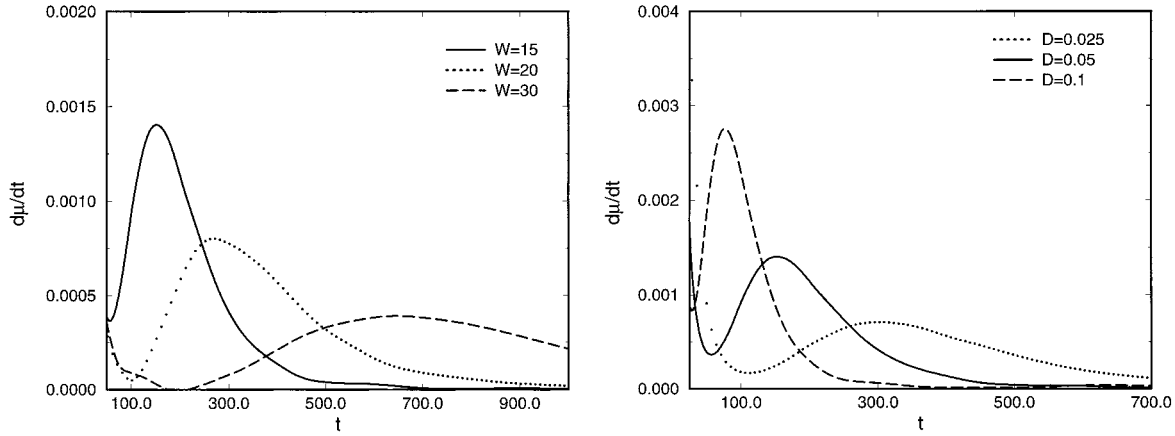

Figure 5. Temporal evolution of the first derivative of the exponent μ with respect to time for two-dimensional tubes for the cases shown in Figure 3. The crossover times $t_{2\rightarrow1}$ are found from the maxima of dμ/dt. Table 1 contains these results.

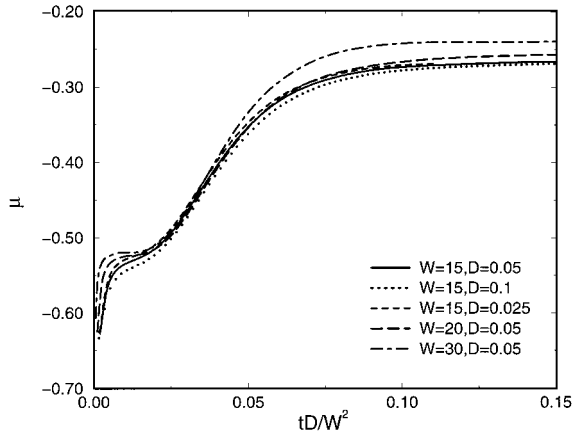

Figure 6. Exponent $\mu(t)$ for two-dimensional tubes shown in Figure 3 but now as a function of scaled time.

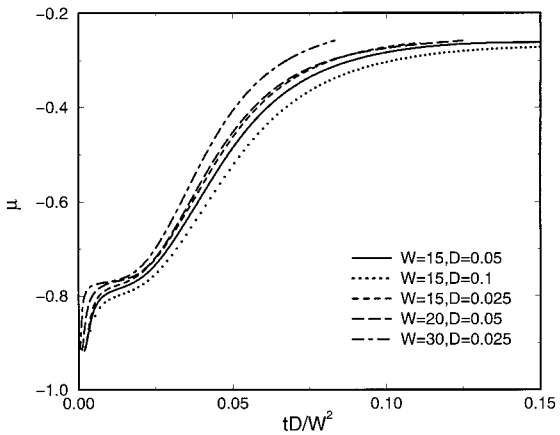

Figure 7. Exponent $\mu(t)$ for three-dimensional tubes of square cross section as a function of scaled time. The size of the tubes is 1000 × W × W and each curve is an average over 10 realizations.

simulations. In one we fix D at 0.05 and vary W_z, and in the other we fix W_z at 15 and vary D. In all cases we take $W_z < W_y$, so that the first crossover ($t_{3\rightarrow2}$) takes place when the aggregates reach the z boundary and the second ($t_{2\rightarrow1}$) when they reach the y boundary. The results of the simulations are shown in Figure 9. In all cases we see the "induction" period toward three-dimensional OZ behavior, a transition to two-dimensional OZ behavior, followed by the onset of another transition toward one-dimensional behavior. The one-dimensional plateau is reached beyond the times shown in the figure. The scaling is in D/W_z^2 since W_y is held fixed.

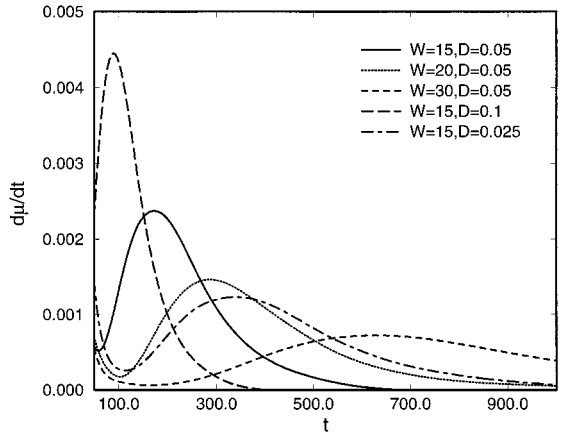

Figure 8. Temporal evolution of the first derivative of the exponent μ with respect to time for the cases shown in Figure 7. The crossover times $t_{3\rightarrow1}$ are found from the maxima of dμ/dt. Table 1 contains these results.

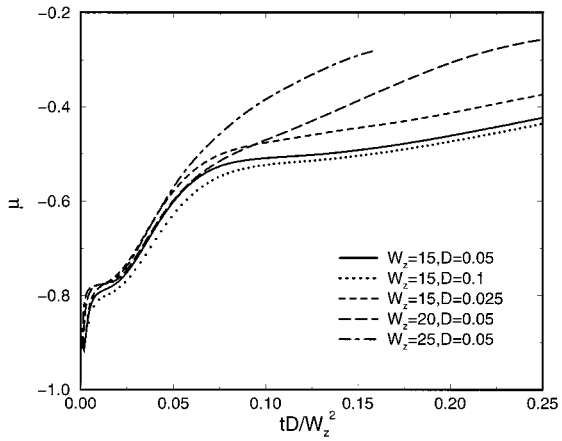

Figure 9. Exponent $\mu(t)$ for three-dimensional tubes of rectangular cross section as a function of scaled time. The size of the tubes is 1000 × W_y × W_z and W_y = 40 in all cases. Each curve is an average over five realizations.

The crossover times $t_{3\rightarrow2}$ and $t_{2\rightarrow1}$ from 3d to 2d OZ behavior and from 2d to 1d OZ behavior respectively are again determined from the maximum values of dμ/dt. We have ascertained that the curves exhibit two maxima. Those associated with the first crossover are tabulated in Table 1. The scaled times are again nearly constant with a value of about 0.035. The second crossover times not shown in the table are also in excellent agreement with the results exhibited.

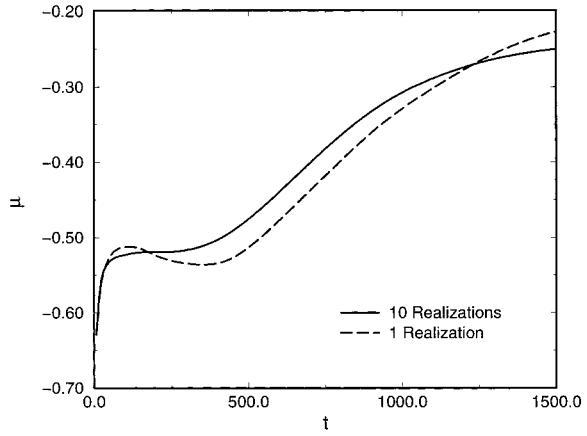

Figure 10. We compare one realization of the $W = 30$-curve in Figure 3 with the 10-realization average.

We end this section with a commentary on some puzzling results in the Monte Carlo simulations of Ahn et al.[5] that they are not able to explain and that we believe are entirely statistical artifacts. In nearly all of their simulation results for the kinetic exponent, upon reaching the plateau value appropriate for OZ behavior in a particular dimensionality their exponent first becomes *more negative* ("overshoots") before proceeding to the next crossover toward a *less negative* value appropriate to a lower dimensionality. We see no such behavior: all of our kinetic exponents behave monotonically with time, as one would expect.

We confirmed the conclusions of Li[4] that this overshoot is not related to boundary conditions (reflective vs periodic).

Since the overshoot seems to be more pronounced for larger systems, we conjecture that it is a statistical problem, despite the fact that Ahn et al.[5] present curves that are averaged over many realizations (but perhaps not enough of them to smooth out this artifact, as they are not enough to smooth out other noisy results). To support this conjecture we compared single realizations in our reaction−diffusion approach with the corresponding curves averaged over 10 realizations, not a large number but sufficient for all practical purposes. We carried out these comparisons for many geometries (two-dimensional tubes, three-dimensional square and rectangular tubes), different initial conditions, and different boundary conditions. In very many cases we found results typified by Figure 10. Any single realization often shows an "overshoot" and/or an "undershoot". Upon averaging, these nonmonotonicities average out and the resulting curve is monotonic as one would expect.

4. Theoretical Analysis

Although the reaction−diffusion system (eq 1) cannot be solved exactly analytically, we have argued elsewhere[6,8,9] that for most initial conditions an analytic solution for the global density and hence for the kinetic exponent accurate for almost all times *can* in fact be found as follows.

We introduce the difference and sum densities

$$\gamma(\mathbf{r},t) = \frac{\rho_A(\mathbf{r},t) - \rho_B(\mathbf{r},t)}{2}$$

$$\rho(\mathbf{r},t) = \frac{\rho_A(\mathbf{r},t) + \rho_B(\mathbf{r},t)}{2} \tag{4}$$

The two parts of eq 1 transform into

$$\frac{\partial}{\partial t}\gamma = D\nabla^2\gamma \tag{5}$$

$$\frac{\partial}{\partial t}\rho = D\nabla^2\rho - K(\rho^2 - \gamma^2) \tag{6}$$

An average of eq 6 over the system volume and over the initial distribution of reactants, indicated by brackets $\langle ... \rangle$, gives

$$\frac{\partial}{\partial t}\langle\rho\rangle = -K(\langle\rho^2\rangle - \langle\gamma^2\rangle) \tag{7}$$

Equation 5 for the difference variable is a simple linear diffusion equation that can be solved trivially:

$$\gamma(\mathbf{r},t) = \frac{1}{V}\sum_{\mathbf{k}}\int d\mathbf{r}' e^{-i\mathbf{k}\cdot(\mathbf{r}-\mathbf{r}')}e^{-Dk^2t}\gamma(\mathbf{r}',0) \tag{8}$$

where $V = \prod_i L_i = L_x L_y ...$ is the system volume and L_i is the length of the edge of the volume in direction i. For periodic boundary conditions, the vector $\mathbf{k}$ has components $k_i = 2\pi n_i/L_i$ where the integer n_i ranges from $-\infty$ to ∞. The mean square average of $\gamma(\mathbf{r},t)$ can be constructed directly from this solution, and for a random initial distribution of reactants the result is[6]

$$\langle\gamma^2(\mathbf{r},t)\rangle = -\frac{\rho(0)}{2V} + \frac{\rho(0)}{2}\prod_i S_i \tag{9}$$

where the first term simply ensures the absence of a uniform background as required under stoichiometric conditions and where

$$S_i \equiv \frac{1}{L_i}\sum_{n_i=-\infty}^{\infty} e^{-8\pi^2 D n_i^2 t/L_i^2} \tag{10}$$

Equation 9 is the last term on the right-hand side of eq 7. The remainder of the analysis depends on the relation between $\langle\rho^2\rangle$ and the global density $\rho(t) = \langle\rho\rangle$. In our earlier work[6,8,9] we argued that for almost all distributions of interest, including those of interest in this work, $\langle\rho^2\rangle \approx \rho^2(t)$. In almost all cases the difference between $\langle\rho^2\rangle$ and $\rho^2(t)$ is of higher order than the leading contributions to either. An exception is the random distribution (which is in fact our initial distribution), but the initial distribution remains random for only an extremely short time in constrained geometries ($d < 4$). As soon as segregation effects begin to set in the equality of the square of the average and the average of the square becomes extremely accurate. We thus invoke this relation for our further analysis and replace eq 7 with

$$\frac{\partial}{\partial t}\rho(t) = -K(\rho^2(t) - \langle\gamma^2\rangle) \tag{11}$$

This is a closed nonlinear differential equation for the global density $\rho(t)$.

The next step in our argument relies on the fact that for $d < 4$ the inhomogeneous term $\langle\gamma^2\rangle$ decays no more rapidly than $t^{-d/2}$. This has been shown in our earlier work[6,8,9] and is also obtained explicitly below. It then follows that the slowest term in the decay of $\rho^2(t)$ must be the same as that of $\langle\gamma^2\rangle$ since otherwise there is no possible source of cancellation of the slowly decaying $\langle\gamma^2\rangle$ contribution. Furthermore, if $\rho^2(t)$ decays no more rapidly than $t^{-d/2}$ it follows immediately that $d\rho/dt$ decays more rapidly than ρ^2. This then leads to the conclusion that the left-hand side of eq 11 is negligible compared to the

other terms. For our further analysis we thus invoke the relation to leading order

$$\rho(t) = \langle \gamma^2(\mathbf{r},t)\rangle^{1/2} = \left(-\frac{\rho(0)}{2V} + \frac{\rho(0)}{2}\prod_i S_i \right)^{1/2} \qquad (12)$$

In all our systems we take the initial density $\rho(0) = 1$.

For our two-dimensional tubes $L_x = L$ and $L_y = W$. For the three-dimensional systems $L_x = L$, $L_y = W_y$, $L_z = W_z$, and in the case of a square cross section $W_y = W_z = W$. In all our systems we take L to be sufficiently large that we can consider it to be infinite, $L \to \infty$, and hence we can convert the corresponding sum to an integral. This immediately leads to[6]

$$S_x = \lim_{L\to\infty} \frac{1}{L}\sum_{n=-\infty}^{\infty} \mathrm{e}^{-8\pi^2 D n^2 t/L^2} \to \int_{-\infty}^{\infty} \mathrm{d}y \mathrm{e}^{-8\pi^2 D t y^2} = \frac{1}{(8\pi D t)^{1/2}} \qquad (13)$$

This leaves us with the discrete sum along each direction of finite size. It is further useful to note that each discrete sum can be written in two equivalent forms, the second obtained from the original form by Laplace transforming the original series 10 with respect to t, reexpressing the resulting sum according to formula 1.217.1 in Gradshteyn and Ryzhik,[10] and then inverse Laplace transforming:

$$S \equiv \frac{1}{W}\sum_{n=-\infty}^{\infty} \mathrm{e}^{-8\pi^2 D n^2 t/W^2} = \frac{1}{(8\pi D t)^{1/2}}\sum_{n=-\infty}^{\infty} \mathrm{e}^{-W^2 n^2/8Dt} \qquad (14)$$

The first form converges rapidly for long times, while the second converges rapidly for short times.

Let us specifically consider two-dimensional tubes. Our analytic expression for the global density is then

$$\rho(t) = \left(\frac{1}{2(8\pi D t)^{1/2}} \frac{1}{W}\sum_{n=-\infty}^{\infty} \mathrm{e}^{-8\pi^2 D n^2 t/W^2} \right)^{1/2} = \left(\frac{1}{16\pi D t}\sum_{n=-\infty}^{\infty} \mathrm{e}^{-W^2 n^2/8Dt} \right)^{1/2} \qquad (15)$$

The first line is most useful for long times, when the dynamics approaches one-dimensional OZ with the associated kinetic exponent $-1/4$, and the second is most useful for short times, when the kinetic exponent is near the two-dimensional value $-1/2$. In general, with eq 3 we now have analytic series expressions for $\mu(t)$.

Either of our series reproduces the numerical results to great accuracy. In Figure 11 we show a typical comparison between our simulation results and the outcome of our analytic series for the kinetic exponent $\mu(t)$. The agreement between the two extends down to the earliest times below which the equality 12 breaks down. The persistent difference between the two essentially parallel curves can be decreased by increasing the rate coefficient K: we have ascertained that the numerical simulation curve moves up toward the analytic curve as K increases, again confirming the validity of assumption 12 for diffusion-limited reactions except at the very earliest times. Similar agreement is obtained using the "short time" analytic series expression. In Figure 12 we exhibit the derivative of the kinetic exponent for the curves in Figure 11. The maxima (and hence the crossover times from OZ-2d to OZ-1d behavior) clearly agree. The precise value of the maximum obtained from the series is $t_{2\to1}D/W^2 = 0.034$.

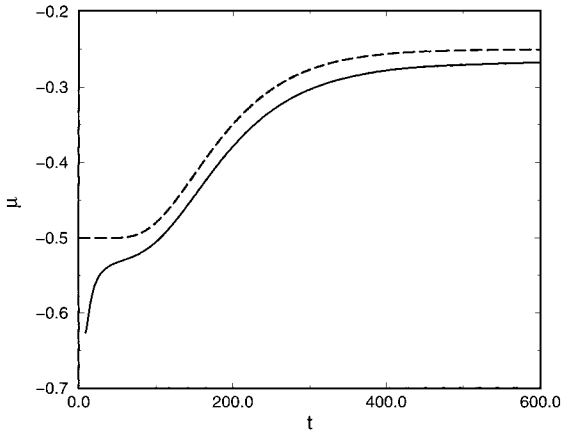

Figure 11. Solid curve: numerical integration results for the kinetic exponent $\mu(t)$ for a two-dimensional tube of width $W = 30$. Dashed curve: result obtained using the first line of eq 15 including 1000 terms in the series. The initial difference between the two curves reflects the "induction" period from classical to OZ-2d behavior.

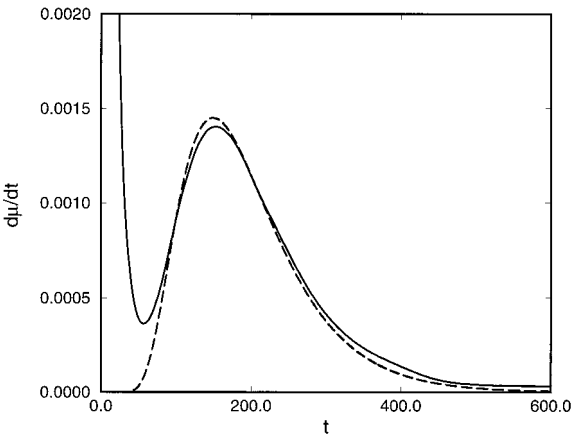

Figure 12. Solid curve: derivative of the solid curve in Figure 11. The maximum in the curve identifies the crossover time from OZ-2d to OZ-1d behavior and corresponds to the first entry in the third column of Table 1. Dashed curve: derivative of our analytic curve in Figure 11.

Remarkably, the crossover time is quite accurately obtained from *either* series by retaining only the $n = 0$ and $n = \pm 1$ terms. Thus, if we set

$$\mu(t) = -\frac{1}{4} + \frac{1}{2}\frac{\mathrm{d}}{\mathrm{d}\log t}\log \sum_{n=-\infty}^{\infty} \mathrm{e}^{-8\pi^2 D n^2 t/W^2} \approx -\frac{1}{4} + \frac{1}{2}\frac{\mathrm{d}}{\mathrm{d}\log t}\log(1 + 2\mathrm{e}^{-8\pi^2 D t/W^2}) \qquad (16)$$

and solve for the time at which $\mathrm{d}^2\mu/\mathrm{d}t^2 = 0$, we find

$$\frac{D}{W^2} t_{2\to1} = 0.0336 \qquad (17)$$

On the other hand, if we set

$$\mu(t) = -\frac{1}{2} + \frac{1}{2}\frac{\mathrm{d}}{\mathrm{d}\log t}\log \sum_{n=-\infty}^{\infty} \mathrm{e}^{-W^2 n^2/8Dt} \approx -\frac{1}{2} + \frac{1}{2}\frac{\mathrm{d}}{\mathrm{d}\log t}\log(1 + 2\mathrm{e}^{-W^2/8Dt}) \qquad (18)$$

we find

$$\frac{D}{W^2}t_{2\to 1} = 0.0331 \tag{19}$$

The agreement with the simulation results is excellent (and can obviously be further improved by retaining more terms in either series).

For three-dimensional tubes of square cross section the corresponding analysis leads to

$$\mu(t) = -\frac{1}{4} + \frac{\mathrm{d}}{\mathrm{d}\log t}\log \sum_{n=-\infty}^{\infty} \mathrm{e}^{-8\pi^2 D n^2 t/W^2}$$

$$= -\frac{1}{2} + \frac{\mathrm{d}}{\mathrm{d}\log t}\log \sum_{n=-\infty}^{\infty} \mathrm{e}^{-W^2 n^2/8Dt} \tag{20}$$

Although the kinetic exponent here is different from that of the two-dimensional tube (as of course it should be), the condition for identifying the crossover time $\mathrm{d}^2\mu/\mathrm{d}t^2 = 0$ leads to exactly the same result for $t_{3\to 1}$ as for $t_{2\to 1}$. The numerical crossover times for this case are slightly larger (see Table 1) for reasons that are not entirely clear, but the agreement is still excellent. For three-dimensional tubes of rectangular cross section

$$\mu(t) = -\frac{1}{4} + \frac{1}{2}\frac{\mathrm{d}}{\mathrm{d}\log t}\log \sum_{n=-\infty}^{\infty} \mathrm{e}^{-8\pi^2 D n^2 t/W_y^2} + \frac{\mathrm{d}}{\mathrm{d}\log t}\log\frac{1}{2}\sum_{n=-\infty}^{\infty} \mathrm{e}^{-8\pi^2 D n^2 t/W_z^2}$$

$$= -\frac{1}{2} + \frac{1}{2}\frac{\mathrm{d}}{\mathrm{d}\log t}\log \sum_{n=-\infty}^{\infty} \mathrm{e}^{-W_y^2 n^2/8Dt} + \frac{1}{2}\frac{\mathrm{d}}{\mathrm{d}\log t}\log \sum_{n=-\infty}^{\infty} \mathrm{e}^{-W_z^2 n^2/8Dt} \tag{21}$$

If W_y and W_z are sufficiently different, e.g., $W_y \gg W_z$ (as they are in our simulations), there is essentially no interference between the maxima associated with each sum and one finds that $t_{3\to 2}D/W_z^2 \approx t_{2\to 1}D/W_y^2 = 0.034$. As W_z and W_y approach one another these crossover times merge to the square cross-section single crossover result.

5. Conclusions

We have investigated the kinetic behavior of the global density $\rho_A(t) = \rho_B(t) = \rho(t)$ as a function of time for the stoichiometric diffusion-limited reaction $A + B \to 0$ in tubular geometries with random initial distributions of reactants. Of particular interest are the transitions of the kinetic exponent $\mu(t) \equiv \mathrm{d}\log\rho(t)/\mathrm{d}\log t$ from Ovchinnikov−Zeldovich (OZ) behavior characteristic of d dimensions to that associated with a lower dimension as the reactants become "aware" of the presence of constraining walls. For two-dimensional tubular geometries we investigated the crossover time $t_{2\to 1}$ from OZ-2d to OZ-1d behavior. In three-dimensional tubes the interesting crossovers are $t_{3\to 1}$ for tubes of square cross section and $t_{3\to 2}$ followed by $t_{2\to 1}$ for tubes of rectangular cross section.

These systems were first investigated using Monte Carlo methods.[5] Despite the very large numbers of particles in very long tubes averaged over extremely large numbers of realizations, the data that emerge from these microscopic simulations are very noisy. At best the data support the expectation that the crossover times scale as $t_{d_1\to d_2} \sim W^2$, where W is the tube width along a narrow direction. This scaling is identified via the intersection point of a straight line fit to the short-time data for the kinetic exponent and another straight line fit to the long-time data. No attempt is made to identify the coefficient(s) in the scaling relation: the data are in any case too noisy for the extraction of such quantitative information. Furthermore, even though one expects the kinetic exponent to vary monotonically with time, the Monte Carlo simulations exhibit nonmonotonicities ("overshoots") that appear to have no clear explanation.

Here we have analyzed these systems using a mesoscopic approach, namely, a reaction−diffusion model, and we have thereby avoided most of the Monte Carlo difficulties. As long as one is not looking at extremely short distance and time scales or extremely low densities, the reaction−diffusion model is known to reproduce the microscopic results extremely accurately.[6] Small differences due to the finite reaction rate coefficient K in the reaction−diffusion model as opposed to the infinite value implicit in the Monte Carlo simulation are ameliorated to any desired degree by taking K to be very large. The average already inherent in the reaction−diffusion approach achieves to a large extent the average over huge numbers of runs that are necessary at the Monte Carlo level, and we find that 5−10 realizations over different initial conditions are sufficient to obtain quantitatively smooth and robust results.

One clear conclusion of our results is that the kinetic exponents $\mu(t)$ are indeed monotonic in all cases. We argue that the "overshoots" in the Monte Carlo results are statistical artifacts of insufficient averaging. Many single reaction−diffusion realizations show similar oscillations, but they average out very quickly (≈5 realizations).

The principal positive outcome of this work is our ability to obtain the kinetic exponent with no noisy distortions, and our ability to obtain quantitative crossover times from one type of OZ behavior to another. Because our results are so smooth and robust, we are able to explore different crossover measures and conclude that the intersection point of linear fits to early and late time behavior of $\mu(t)$ is not the best measure. Instead, we choose the time at which $\mu(t)$ has its maximum curvature, i.e., the time at which $\mathrm{d}^2\mu(t)/\mathrm{d}t^2 = 0$. This criterion of course requires smooth and robust data for $\mu(t)$. In Table 1 we show the results, which are essentially constant over a variety of geometries and parameter values when properly scaled. Our theoretical analysis leads to our prediction for these crossover times, universally denoted by t_c:

$$t_c = 0.034\frac{W^2}{D} \tag{22}$$

where D is the diffusion constant of either species. This is in excellent agreement with our numerical results.

Finally, it is interesting to speculate on the significance of the coefficient 0.034. It is in line with the coefficient associated with the mean first passage time for a diffusive process with random initial conditions to arrive at the wall: this time is given by $t_1 = W^2/24D = 0.041W^2/D$.[11]

Acknowledgment. R.R. gratefully acknowledges the support of this research by the Ministerio de Educación y Cultura through Postdoctoral Grant PF-98-46573147. This work was supported in part by the U.S. Department of Energy under Grant DE-FG03-86ER13606.

References and Notes

(1) Ovchinnikov, A. A.; Zeldovich, Y. G. *Chem. Phys.* **1978**, *28*, 215.
(2) Kang, K.; Redner, R. *Phys. Rev. Lett.* **1984**, *52*, 955.

(3) Lin, A. L.; Kopelman, R. *Phys. Rev. E* **1996**, *54*, R5893.
(4) Li, J. *Phys. Rev. E* **1997**, *55*, 6646.
(5) Ahn, J.; Kopelman, R.; Argyrakis, P. *J. Chem. Phys.* **1999**, *110*, 2116.
(6) Lindenberg, K.; Argyrakis, P.; Kopelman, R. In *Fluctuations and Order: The New Synthesis*; Millonas, M., Ed.; Springer: Berlin, 1996; p 171.
(7) Reigada, R. *Effects of Some Mixing Flows on Diffusion-Controlled Reactions*, Ph.D. Thesis, Universitat de Barcelona, November 1997. Reigada, R.; Sagues, F.; Sokolov, I. M.; Sancho, J. M.; Blumen, A. *Phys. Rev. E* **1996**, *53*, 3167.
(8) Sancho, J. M.; Romero, A. H.; Lindenberg, K.; Sagues, F.; Reigada, R.; Lacasta, A. M. *J. Phys. Chem.* **1996**, *100*, 19066.
(9) Lindenberg, K.; Romero, A. H.; Sancho, J. M. *International Journal of Bifurcation and Chaos* **1998**, *8*, 853.
(10) Gradshteyn, I. S.; Ryzhik, I. M. *Table of Integrals, Series and Products*; Academic Press: New York, 1965.
(11) Seshadri, V.; Lindenberg, K. *J. Stat. Phys.* **1980**, *22*, 69.